

Selection of a powder for ceramic injection moulding

R. E. F. Q. NOGUEIRA, M. J. EDIRISINGHE*, D. T. GAWNE

Department of Materials Technology, Brunel University, Uxbridge, Middlesex UB8 3PH, UK

Ceramic suspensions were prepared from six alumina powders using the same high molecular weight organic vehicle. 18 mm diameter cylinders were compression moulded from four of these suspensions which were suitable for ceramic injection moulding. The organic vehicle in each cylinder was removed by thermal degradation according to the same temperature ramp. The defects present in the cylinders after removal of the organic vehicle are discussed in terms of the powder characteristics. Criteria for the selection of ceramic powders that could be used together with a high molecular weight organic vehicle for this shape-forming method, are deduced from the results obtained.

1. Introduction

The presence of strength-limiting defects introduced during shape-forming operations is a major cause in preventing full exploitation of engineering ceramic materials [1, 2], and this has led to extensive research in this area during the last decade. Injection moulding is a very attractive shaping method because it allows mass production of complex components with high dimensional accuracy and good process control [3, 4]. In this process the ceramic powder is usually dispersed in a polymeric vehicle [3] which allows it to be injected into a shape-forming die cavity. Subsequently, the organic vehicle is removed, mainly by slow heating [4], before sintering the ceramic.

The major aim of most investigations on ceramic injection moulding has been the development of selection criteria for the organic vehicle: good dispersion of the ceramic powder [5], acceptable flow behaviour [6] and rapid removal without creating defects in the ceramic [4]. The last criterion has been the most difficult to satisfy and modelling the removal of the organic vehicle has been investigated by several workers [7-11] to develop a more fundamental understanding about this stage of the process. However, success has been limited and fabrication of thick sections (> 10-15 mm) remains a problem due to high scrap rates during removal of the organic vehicle [12].

The influence of the ceramic powder on the various stages of the process has been largely ignored in the literature. However, recent research has revealed that powder characteristics could (i) influence green microstructure [13], (ii) catalyse organic vehicle pyrolysis [14], and (iii) affect the creation of defects during removal of the organic vehicle [15]. It was significant that, under identical conditions, successful removal of the same high molecular weight organic vehicle from 18 mm diameter cylinders was dependent on the particle size of the ceramic powder present [15]. In this instance, cylinders containing A16.SG alumina with a

median particle size of 0.4 μm (surface area 9.5 $\text{m}^2 \text{g}^{-1}$) were bloated after removal of the organic vehicle. Identical mouldings containing MA2LS alumina with a similar shape particle-size distribution but a median particle size of 6 μm (surface area 0.3 $\text{m}^2 \text{g}^{-1}$), remained macro-defect free. Obstruction to thermal degradation products diffusing out during the removal of the organic vehicle due to different levels of powder packing is a major reason for this [15].

In the present work, several alumina powders with particle-size distributions ranging between those of the MA2LS and A16.SG alumina [15] have been used to prepare suspensions containing a polypropylene organic vehicle. Suspensions suitable for ceramic injection moulding were used to compression mould identical cylinders from which the organic vehicle was removed by thermal degradation. The defects present in these cylinders after the removal of the organic vehicle are explained in terms of the characteristics of the powder present. Overall, these results highlight the powder characteristics that should accompany a high molecular weight polymeric vehicle in order that successful compounding, moulding, removal of organic vehicle and sintering can be carried out to produce macro-defect-free thick section components.

2. Experimental procedure

2.1. Materials

The sources, compositions and surface areas of the alumina powders used are given in Table I. The particle-size distribution and particle morphology of each powder are given in Figs 1 and 2, respectively.

The organic vehicle consisted of isotactic polypropylene, atactic polypropylene and stearic acid in the weight ratio 4:4:1. Sources and other details of each constituent are given in Table II. The small amount of stearic acid acts as a surfactant [16] improving the wettability between the ceramic powder and the polypropylene.

* Author to whom all correspondence should be addressed.

2.2. Mixing and compounding

Each ceramic powder and stearic acid were first mixed together by tumbling in a container. Subsequently, polypropylene was added and mixing continued for

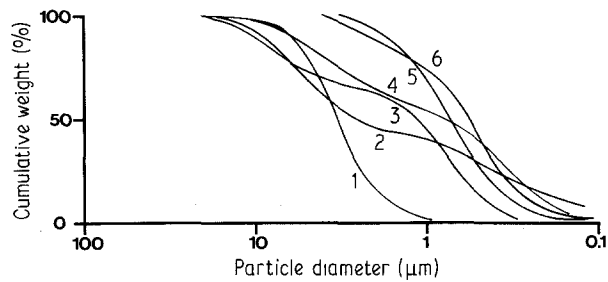


Figure 1 Particle-size distribution of each alumina powder. 1, MA; 2, MA250(5); 3, MA250(2); 4, MA250(3); 5, A152.SG; 6, CT 2000.SG.

~ 5 min. Initially, 60 vol% ceramic powder was added and blends were prepared in 1.5 kg batches.

Compounding of the blends was done using an intermeshing, co-rotating twin-screw extruder (Betol Machinery, Luton, Bedfordshire, UK). Details about the extruder are published elsewhere [17]. Table III shows the compounding conditions. Similar conditions have previously been successful for this organic vehicle [18].

The extrudate of each suspension was water cooled and dried under vacuum before being granulated. Some blends were difficult to extrude according to the conditions given in Table III and were diluted by adding more organic vehicle to reduce the volume percentage of ceramic.

2.3. Compositions

At least four samples of each suspension prepared

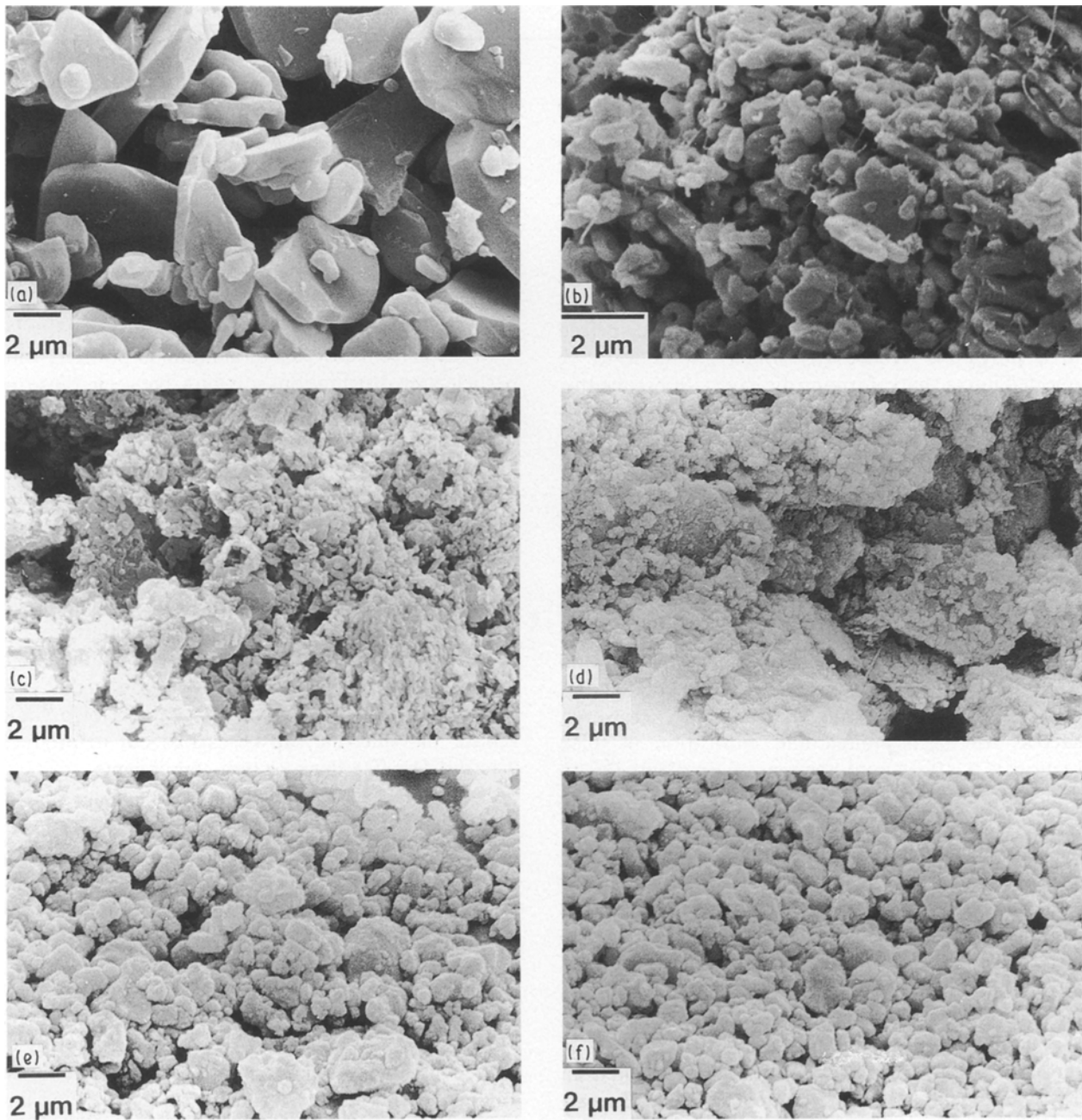


Figure 2 Scanning electron micrographs of the alumina powders. (a) MA, (b) MA250(2), (c) MA250(3), (d) MA250(5), (e) A152.SG, (f) CT2000.SG.

TABLE I Details of the alumina powders used

Type	Source	Surface area (m ² g ⁻¹)	Major impurities (wt %)		
			Na ₂ O	SiO ₂	Fe ₂ O ₃
MA	BA Chemicals Ltd, Gerrards Cross, UK	1	0.4	0.03	0.02
MA250(2)	BA Chemicals Ltd	3.5	0.4	0.03	0.02
MA250(3)	BA Chemicals Ltd	5.5	0.4	0.03	0.02
MA250(5)	BA Chemicals Ltd	> 10	0.4	0.03	0.02
A152.SG	Alcoa Manufacturing (GB) Ltd, Worcester, UK	3	0.04	0.05	0.04
CT2000.SG	Alcoa Manufacturing (GB) Ltd	4.3	0.08	0.06	0.02

TABLE II Details of the organic vehicle constituents

Constituent	Source	Density (kg m ⁻³)	Molecular weight (\bar{M}_n)
Grade GY545M isotactic polypropylene	ICI Ltd, Welwyn Garden City, UK	905	31850
Grade MF5 atactic polypropylene	APP Chemicals Salop, UK	870	2865
Stearic acid	BDH Chemicals Ltd, Poole, UK	941	Relative molecular mass = 284

TABLE III Compounding conditions

Screw diameter (mm)	40
Screw length/diameter ratio	17
Screw speed (r.p.m.)	60
Barrel temperature profile (feed to exit, °C)	180–180–190–190

were ashed at 600 °C to estimate the exact volume percentage of ceramic present. Ashed samples of all suspensions were subjected to iron analysis by absorption spectroscopy using an SP1800 double-beam spectrometer. Details of each suspension prepared are given in Table IV.

2.4. Moulding

Cylinders, 18 mm diameter and nominally 30 mm long, were compression moulded from compositions 1, 2, 7 and 8 (Table IV) at 200 °C under a pressure of 12 MPa using an Apex model M1/R press (Apex Construction Ltd, Dartford, UK). The cylinders were X-ray radiographed using a Hewlett Packard Faxitron contact radiography camera. Compression moulding was used instead of injection moulding because the former technique is more feasible for fabricating simple shapes from a small quantity of material.

2.5. Removal of the organic vehicle

The cylinders were heated in flowing oxygen-free nitrogen according to the ramp shown in Fig. 3 to remove the organic vehicle. Subsequently, the cylinders were X-ray radiographed.

2.6. Sintering

The sinterability of MA, MA250(2), A152.SG and CT2000.SG alumina powders in compositions 1, 2, 7

and 8, respectively, was assessed using pressed bars having nominal dimensions 50 mm × 8 mm × 5 mm. A Dension testing machine was used in the compression mode to press the bars under a pressure of 125 MPa. The densities of the bars were measured by mercury immersion. Subsequently, the bars were sintered by heating to 1650 °C and soaking at this temperature for 2 h. The densities of the sintered samples were also measured using mercury immersion.

3. Results and discussion

3.1. Powder characteristics

Three of the powders used in this investigation, MA250(1), MA250(2) and MA250(3), have approximately similar wide, multimodal particle-size distributions with median particle size between 1 and 2 μm (Fig. 1). These powders have an oblong particle shape and are agglomerated (Fig. 2). In contrast, MA, A152.SG and CT2000.SG alumina powders have relatively narrow, monomodal particle-size distributions (Fig. 1). CT2000.SG contains a higher proportion of sub-micrometre particles compared to A152.SG and has the highest surface area (Table I). Both CT2000.SG and A152.SG have an equiaxed particle shape and are much less agglomerated compared to the MA250 type powders (Fig. 2). MA is a coarse powder with particles > 1 μm in size. It has a platelet-like particle shape (Fig. 2) and the lowest surface area (Table I).

3.2. Organic vehicle

The flow properties of the isotactic polypropylene–atactic polypropylene–stearic acid organic vehicle are acceptable for injection moulding [18]. The incorporation of microcrystalline wax for atactic polypropylene enhances the flow properties further [6, 18]. However, in terms of removal of the organic vehicle from

TABLE IV Composition and other details of suspensions prepared. Standard deviations are given in parenthesis. Wt % iron values shown have been corrected to exclude the iron content in the as-received powders

No.	Ceramic powder	Behaviour during Compounding	Vol % Ceramic (by ashing)	Wt % iron take up
1	MA	Extruded easily	60 (0.23)	0.004
2	MA250(2)	Extruded fairly well	60 (0.18)	0.286
3	MA250(2)	Extruded easily	52 (0.01)	0.016
4	MA250(3)	Very difficult to extrude	56 (0.18)	0.576
5	MA250(3)	Extruded fairly well	53 (0.06)	0.176
6	MA250(5)	Very difficult to extrude	53 (0.13)	0.286
7	A152.SG	Extruded easily	58 (0.01)	—
8	CT2000.SG	Extruded easily	59 (0.03)	—

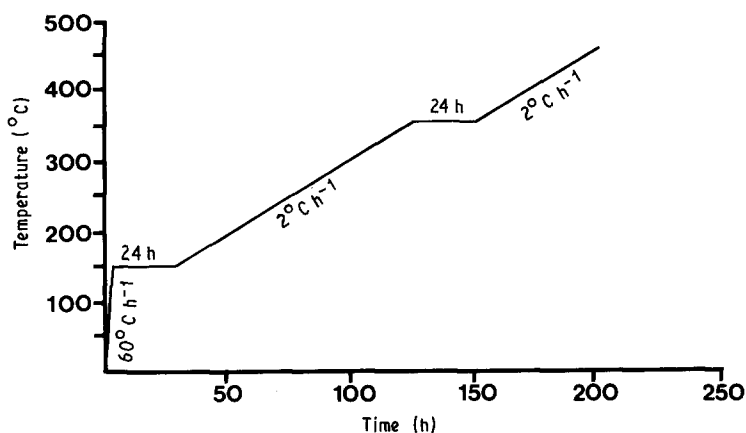


Figure 3 The temperature-time schedule used for removal of the organic vehicle.

thick sections, the isotactic polypropylene-atactic polypropylene-stearic acid system gives better results [19] and, therefore, has been favoured in this investigation in preference to the 6:2:1 weight ratio isotactic polypropylene-microcrystalline wax-stearic acid system used in our previous work. In addition, atactic polypropylene has a smaller per cent crystallinity and therefore causes a lower shrinkage on moulding reducing the possibility of shrinkage-related defects [20].

3.3. Suspensions prepared

The incorporation of these powders in an organic vehicle involves particle packing and in this respect the powders with a wide, multimodal particle-size distribution could be expected to give a high solids loading without a dramatic increase in viscosity [21]. However, Table IV indicates that this was not the case and, in fact, MA250(5) could only be extruded with difficulty at 53 vol % ceramic, taking up approximately 0.3 wt % iron during the operation. Agglomeration is the major cause for this as it reduces particle packing [22] and increases the suspension viscosity [23]. As agglomeration decreased (Fig. 2), first in MA250(3) and then further in MA250(2) it was possible to incorporate a similar volume percentage of ceramic in the extruded suspensions with a smaller weight per cent iron take up (Table IV). In fact, it was possible to increase the volume percentage of ceramic in the MA250(2) suspension to 60, although approximately 0.3 wt % iron, exactly the same as the suspension containing 53 vol % MA250(5), was present in the extrudate (Table IV).

A spherical particle shape causes the most efficient particle packing [24]. Thus A152.SG and CT2000.SG, both with an equiaxed, near-spherical particle shape, extruded very easily at approximately 60 vol % ceramic with undetectable iron take up. Deviation of particle morphology from near-spherical to an oblong particle shape reduces packing efficiency [24] and this factor too would have contributed to the difficulties faced in extruding concentrated MA250 alumina powders. Packing efficiency is lowest when a platelet-like particle shape is encountered [24]. In fact, particle morphology has a dramatic effect on particle packing with the maximum volume percentage of solids decreasing from over 60% to 20% when the particle aspect ratio is increased from 1 to 23 in the case of glass-water suspensions [25]. However, the fact that it was possible to easily extrude platelet-shape MA alumina with particles $> 1 \mu\text{m}$ to 60 vol % ceramic (Table IV) suggests that the adverse effect of an unfavourable particle shape could be considerably reduced by having a coarser particle size which improves packing in a suspension [26].

Suspensions suitable for ceramic injection moulding should be as concentrated as possible to reduce slumping and shrinkage during removal of the organic vehicle. In addition, dilute suspensions result in low prefired mechanical strength causing handling problems, and subsequent sintering also suffers from distortion and high shrinkage. Therefore, only those suspensions containing approximately 60 vol % ceramic were used in the organic vehicle removal studies discussed below.

3.4. Removal of organic vehicle

Figures 4a–d show X-ray radiographs of the cylinders made from compositions 1, 2, 7 and 8 (Table IV) before and after removal of the organic vehicle by heating in flowing nitrogen according to the temperature ramp given in Fig. 3. Under these conditions, thermal degradation of the organic vehicle takes place and polypropylene breaks down to smaller fragments [27] which diffuse outwards in the moulded body. In addition, movement of the ceramic particles occurs, causing shrinkage and increasing packing, although maximum packing efficiency, where particle contacts maximize, is not achieved [28].

All four as-moulded cylinders did not contain any macro-cracks or voids (Fig. 4a–d). After removal of the organic vehicle the cylinder containing MA alumina was extensively cracked (Fig. 4a). Most of the cracks occur in a direction parallel to its axis. Further packing of non-spherical particles during removal of the organic vehicle require both the approach of particle centres and rotation [29]. The platelet-like particle morphology of MA alumina shows excessive deviation from sphericity and in this type of situation, particle movement during removal of the organic vehicle is difficult even with capillary pressures helping to cause shrinkage [24]. This restriction in particle movement caused cracking during the removal of the organic vehicle. Compared with MA alumina, the MA2LS alumina used in the earlier investigation [15] had a very similar particle-size distribution with a slightly coarser median particle size. However, its particle shape showed much less deviation from sphericity compared with the characteristic platelet-like shape of MA alumina [30] and this helped in avoiding this type of cracking during removal of the organic vehicle.

The cylinders made from composition 8 containing CT2000.SG alumina show gas porosity (Fig. 4d) after removal of the organic vehicle, similar to the A16.SG alumina in our previous investigation [15]. Clearly, the outward diffusion of degradation products has faced obstruction. However, there is considerably less gas porosity and bloating compared to the A16.SG alumina specimen [15]. Figure 4c shows that in the case of A152.SG alumina cylinder, removal of the organic vehicle did not create any such voids or macro-cracks. A152.SG, CT2000.SG and A16.SG contain equiaxed powder particles which almost approximate to the ideal spherical shape. A16.SG has a narrower particle-size distribution compared to A152.SG [15]. It has a much finer particle size and a specific surface area – about three times that of A152.SG [15]. CT2000.SG is very similar in powder characteristics to A152.SG but has a higher proportion of finer particles (Fig. 1) and therefore about a 40% greater specific surface area than A152.SG (Table I).

A decrease in particle size causes the reduction in the space between particles [31] and this can be further diminished due to the larger surface area of such fine powders adsorbing ~ 100 nm thick immobile organic vehicle layers [32]. Thus, adsorbed layers reduce the “mobile” organic vehicle available for the

diffusion of degradation products. The higher surface area will also give rise to the presence of larger amounts of adsorbed water which has to diffuse through the same space. In this context, a non-polar polymer such as polypropylene is not favourable as the organic vehicle, because water diffuses better through polar polymers such as EVA [33].

It is interesting to compare the influence on diffusion caused by the inclusion of A152.SG, CT2000.SG and A16.SG in the organic vehicle. Using the Bruggeman equation [34]

$$D_e = (1 - V_o)^{1.5} \quad (1)$$

where $V_e = V_c (1 + 0.5\rho_c S_c h)$ as proposed before [15]. D_e is the effective diffusion coefficient which is the ratio between the diffusion coefficients of the suspension and the organic vehicle. V_e is the effective volume fraction of ceramic taking organic vehicle adsorption into account. V_c is the volume fraction of ceramic in the suspension. ρ_c and S_c are the density and specific surface area of the ceramic powder, respectively, while h is the adsorbed layer thickness which for isotactic polypropylene is 14 nm. Taking $\rho_c = 3987 \text{ kg m}^{-3}$ and $S_c = 9.5 \text{ m}^2 \text{ g}^{-1}$ for A16.SG for a 60 vol % ceramic suspension, D_e is 75% and 58% higher in A152.SG and CT2000.SG, respectively, compared to A16.SG. Thus, voids are more likely to form in the CT2000.SG cylinder, compared with A152.SG (Fig. 4c), as observed in this investigation, because the degradation products find more difficulty in outward diffusion. Thus, their concentration in the degrading the organic vehicle increases and when the corresponding vapour pressure is greater than the atmospheric pressure, boiling takes place [10].

The X-ray radiographs of the MA250(2) cylinder (Fig. 4b) emphasize the importance of space between particles during the removal of organic vehicle. Voids and macro-cracks are not present in the MA250(2) cylinder after removal of the organic vehicle. This is a consequence of the oblong particle shape (Fig. 2) which caused less-efficient particle packing compared with the equiaxed, near-spherical powders, as discussed earlier. This leaves a greater amount of inter-particle space for the diffusion of degradation products of the organic vehicle.

It is interesting that similar observations were made when such powders were moulded using the isotactic polypropylene–microcrystalline wax–stearic acid organic vehicle [35]. This suggests that the trends observed in this investigation would be valid for other high molecular weight polymeric organic vehicles. Of course, the problems associated with low molecular weight organic vehicles are different, and lead to other types of particle packing problems [36].

3.5. Sinterability

The relative densities of the as-pressed and as-sintered bars made from MA250(2), MA, A152.SG and CT2000.SG powders are given in Table V. The use of higher pressures during pressing did not help in further increasing the relative densities measured. It is clear that the volume percentage of ceramic in all the pressed bars is lower than that in the extruded suspen-

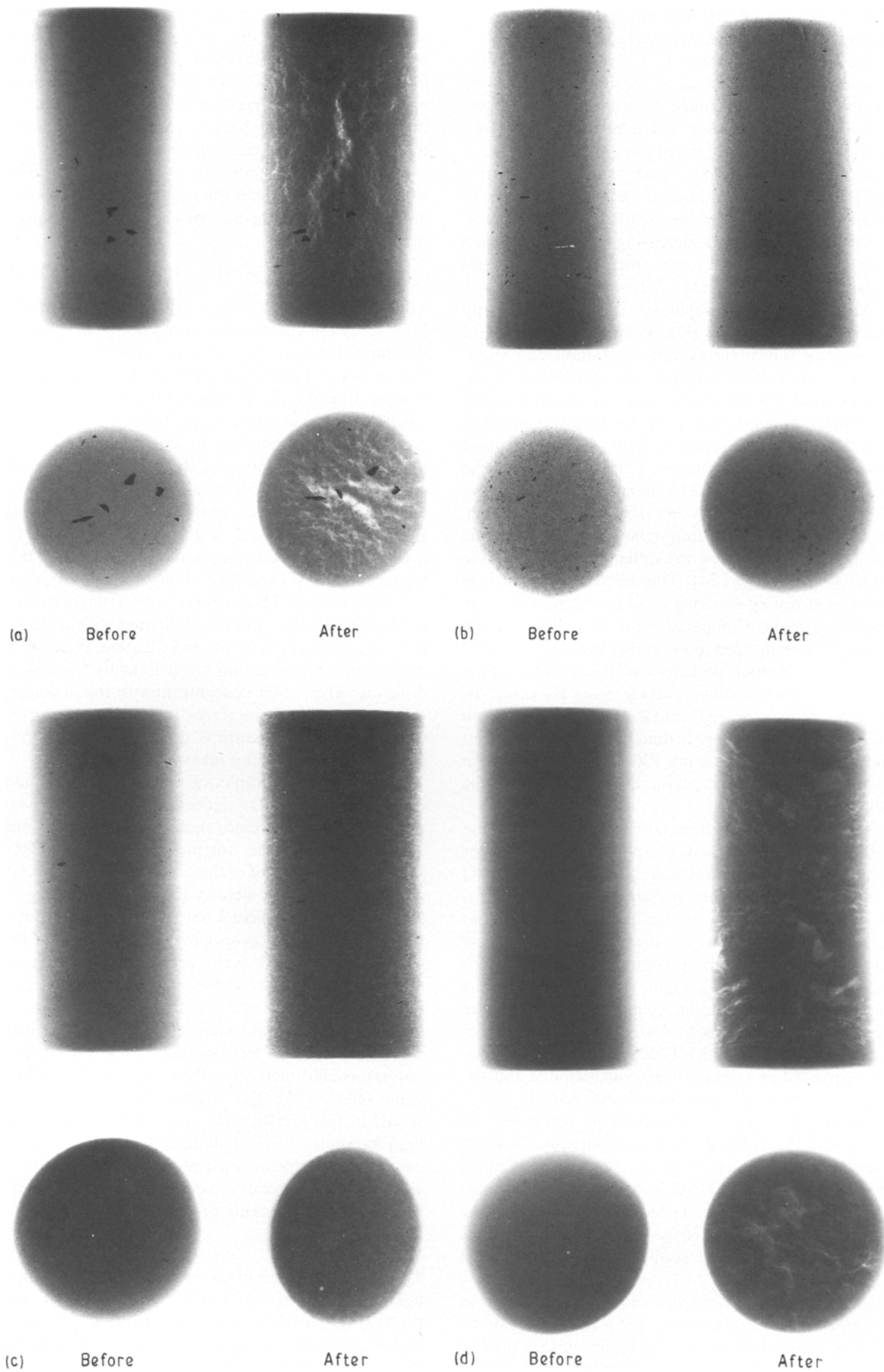


Figure 4 X-ray radiographs of 18 mm diameter cylinders made using compositions (a) 1, (b) 2, (c) 7 and (d) 8 before and after removal of the organic vehicle. Metallic inclusions (due to iron take up) are clearly shown in the radiographs.

TABLE V Relative densities of as-pressed and as-sintered bars

Powder	Relative density (%)	
	As-pressed	As-sintered
MA250(2)	47	70
MA	49	63
A152.SG	54	92
CT2000.SG	53	93

sions especially in the case of the more non-spherical shaped powders MA250(2) and MA. Therefore, in general, dispersing ceramic powders in an organic vehicle allows better packing of particles.

The as-sintered densities achieved without the incorporation of sintering aids clearly shows that both A152.SG and CT2000.SG have superior sinterability and this is due to their finer particle size and a more spherical particle shape. MA alumina, where the particle shape deviated most from sphericity, showed the lowest increase in per cent relative density. MA250(2) showed a larger increase in per cent relative density but was still 30% away from full density. Therefore, although the oblong particle shape of MA250(2) helped the successful removal of the organic vehicle as discussed above, its sintering characteristics make it unfavourable for the final stage of the ceramic injection-moulding process. It is important to note that powders selected for the ceramic injection-moulding process must satisfy all four stages, namely mixing and compounding, moulding, organic vehicle removal and sintering.

4. Conclusions

Particle packing characteristics suitable for all four stages of the process should be carefully considered when selecting ceramic powders for injection-moulding suspensions. Although it is well established that a wide particle-size distribution is preferred for the process in order that a higher volume percentage of ceramic can be incorporated in the organic vehicle, these results have shown that particle shape has considerable influence on the entire process. Overall, under the conditions investigated, a powder with near-spherical particle shape, a median particle size of just under 1 μm corresponding to the particle-size distribution shown by A152.SG alumina, and a specific surface area of $\sim 3 \text{ m}^2 \text{ g}^{-1}$, was most satisfactory for all stages of the process. It helped (i) compounding a concentrated suspension with a low iron take up (ii) successful removal of the organic vehicle without creating voids and macro-cracks, and (iii) to achieve satisfactory sinterability. It is significant that the oblong particle shape of MA250(2) was helpful in the removal of the organic vehicle because of less efficient packing, but it reduced sinterability and, to a lesser extent, made compounding of concentrated suspensions more difficult.

Acknowledgements

The authors thank CNPq, Brazilian Government, for

funding given to R. Nogueira, Mr. L. Mellett for technical support, Leeds Mining Consultants, Kirkstall, Leeds, UK, for iron analysis, and Mrs K. Goddard for typing the manuscript.

References

1. N. ALFORD, K. KENDELL, B. CLEGG and T. BUTTON, *Phys. World* (May) (1991) 26.
2. R. CARLSSON, *Mater. Design* **10** (1989) 10.
3. M. J. EDIRISINGHE and J. R. G. EVANS, *Int. J. High Tech. Ceram.* **2** (1986) 1.
4. *Idem, ibid.* **2** (1986) 249.
5. *Idem, Proc. Brit. Ceram. Soc.* **38** (1986) 67.
6. *Idem, J. Mater. Sci.* **22** (1987) 269.
7. R. M. GERMAN, *Int. J. Powder Metall.* **23** (1987) 237.
8. P. CALVERT and M. CIMA, *J. Amer. Ceram. Soc.* **73** (1990) 575.
9. M. R. BARONE and J. C. ULICNY, *ibid.* **73** (1990) 3323.
10. J. R. G. EVANS, M. J. EDIRISINGHE, J. K. WRIGHT and J. CRANK, *Proc. Roy. Soc. Lond. A* **432** (1991) 321.
11. G. C. STANGLE and I. A. AKSAY, *Chem. Engng Sci.* **45** (1990) 1719.
12. M. J. EDIRISINGHE, *Bull. Amer. Ceram. Soc.* **70** (1991) 824.
13. V. K. PUJARI, *J. Amer. Ceram. Soc.* **72** (1989) 10.
14. S. MASIA, P. D. CALVERT, W. E. RHINE and H. K. BOWEN, *J. Mater. Sci.* **24** (1989) 1907.
15. J. R. G. EVANS and M. J. EDIRISINGHE, *ibid.* **26** (1991) 2081.
16. M. J. EDIRISINGHE, *Ceram. Int.* **17** (1991) 89.
17. M. J. EDIRISINGHE and J. R. G. EVANS, *Ind. Ceram.* **7** (1987) 100.
18. *Idem, Brit. Ceram. Trans. J.* **86** (1987) 18.
19. J. WOODTHORPE, M. J. EDIRISINGHE and J. R. G. EVANS, *J. Mater. Sci.* **24** (1989) 1038.
20. M. J. EDIRISINGHE and J. R. G. EVANS, *ibid.* **22** (1987) 2267.
21. J. A. MANGELS and W. TRELA, in "Advances in Ceramics", Vol. 9, edited by J. Mangels (American Ceramic Society, OH, 1984) p. 220.
22. T. B. LEWIS and L. E. NIELSEN, *Trans. Soc. Rheol.* **12** (1968) 421.
23. B. C. MUTSUDDY, *Proc. Brit. Ceram. Soc.* **33** (1983) 117.
24. V. N. SHUKLA and D. C. HILL, *J. Amer. Ceram. Soc.* **72** (1989) 1797.
25. V. V. JINESCA, *Int. Chem. Engng* **14** (1974) 397.
26. C. PARKINSON, S. MATSUMOTO and P. SHERMAN, *J. Colloid Interface Sci.* **33** (1970) 150.
27. J. K. Y. KIANG, P. C. UDEN and J. C. W. CHIEN, *Polym. Deg. Stab.* **2** (1980) 113.
28. J. K. WRIGHT, M. J. EDIRISINGHE, J. G. ZHANG and J. R. G. EVANS, *J. Amer. Ceram. Soc.* **73** (1990) 2653.
29. W. D. KINGERY, *J. Appl. Phys.* **30** (1959) 301.
30. BA Chemicals Ltd, Gerrards Cross, Bucks, UK, private communication, 5th January, 1989.
31. D. J. CUMBERLAND and R. J. CRAWFORD, "Packing of Particles" (Elsevier, Amsterdam, 1987) p. 60.
32. G. P. BIERWAGEN, *J. Paint Tech.* **44** (1972) 46.
33. C. E. ROGERS, in "Physics and Chemistry of the Organic Solid State", edited by D. Fox, M. A. Labes and A. Weinberger (Interscience, New York, 1965) p. 109.
34. D. A. G. BRUGGEMAN, *Ann. Phys.* **24** (1935) 636.
35. R. E. F. Q. NOGUEIRA and M. J. EDIRISINGHE, in "New Materials and their Applications", edited by D. Holland (Institute of Physics, London, 1990) p. 43.
36. M. J. EDIRISINGHE, K. L. TOMKINS and M. PATCHING, in "Forming Science and Technology for Ceramics", edited by M. J. Cima (American Ceramic Society, OH, 1991) p. 165.

Received 8 October 1991
and accepted 11 February 1992